Cell Reports, Volume *27*

Supplemental Information

Reduced Prefrontal Synaptic Connectivity and Disturbed Oscillatory Population Dynamics in the CNTNAP2 Model of Autism

Maria T. Lazaro, Jiannis Taxidis, Tristan Shuman, Iris Bachmutsky, Taruna Ikrar, Rommel Santos, G. Mark Marcello, Apoorva Mylavarapu, Swasty Chandra, Allison Foreman, Rachna Goli, Duy Tran, Nikhil Sharma, Michelle Azhdam, Hongmei Dong, Katrina Y. Choe, Olga Peñagarikano, Sotiris C. Masmanidis, Bence Rácz, Xiangmin Xu, Daniel H. Geschwind, and Peyman Golshani

Supplementary Fig. 1

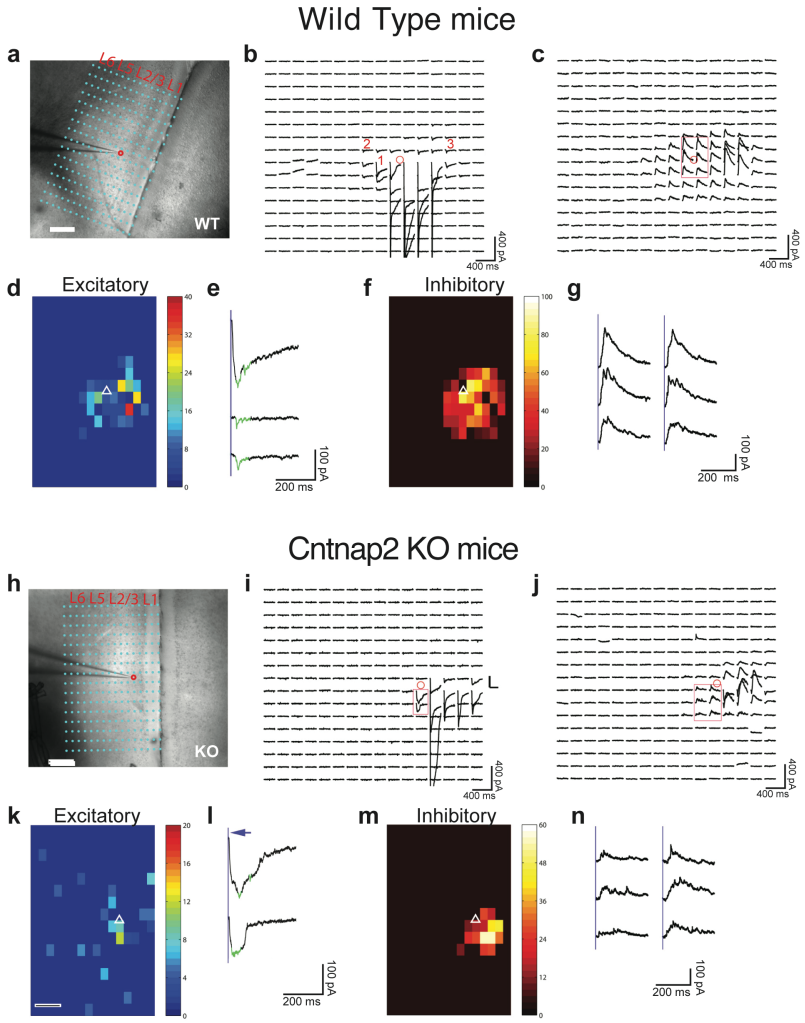

Supplementary Fig. 1 | Example cortical input map data for Cntnap2 WT and KO L2/3 mPFC excitatory neurons. Related to Figure 1. **a**,**h**, Differential interference contrast (DIC) image of mPFC, superimposed with photostimulation sites (cyan dots), spaced at 100 µm x 60 µm, for WT and KO mice. The tip of the patch pipette (recording electrode) and the cell body location of a recorded L2/3 neuron is indicated by a red circle. **b**,**c**,**i**,**j**, Photostimulation-evoked response traces plotted according to their corresponding photostimulation sites, as shown in **a**,**h**. Traces depict currents recorded 250 ms after stimulation (1.5 ms, 15 mW) onset. Cells were voltage-clamped at −70 mV to detect inward excitatory postsynaptic currents (EPSCs), depicted in **b** and **i**, and at +5 mV to detect inhibitory postsynaptic currents (IPSCs), depicted in **c** and **j**. Excitatory **d**,**k** and inhibitory **f**,**m** input maps of average integrated stimulation responses for datasets shown in **b**,**i** and **c**,**j**, respectively. Somatic location of the recorded neuron is represented by a white triangle. **e**,**l** and **g**,**n** show enlarged insets of selected responses in **b**,**i** and **c**,**j**, respectively. Green overlays mark over-riding synaptic responses. Average input amplitudes were calculated as mean integrated amplitudes of EPSCs or IPSCs elicited within the 250 ms post-stimulus onset time-frame. White scale bars represent 250 µm.

Supplementary Fig. 2

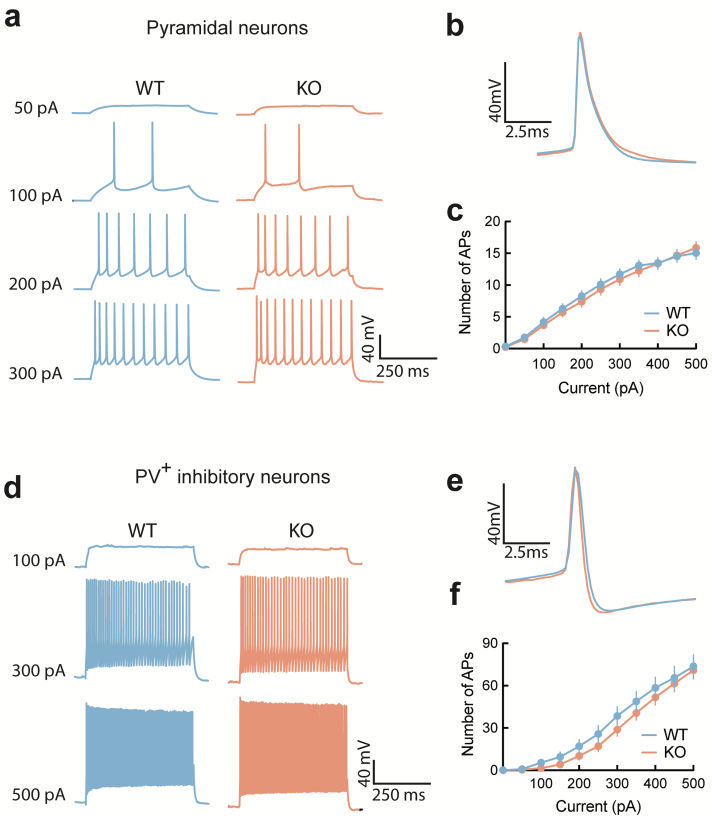

Supplementary Fig. 2 | Intrinsic excitability of L2/3 pyramidal neurons and parvalbumin-positive (PV+) inhibitory neurons in Cntnap2 WT and KO mice. Related to Figure 1. **a**,**d,** Representative action potential traces from L2/3 WT and KO pyramidal and PV+ neurons, showing responses to various current injections and **b**,**e**, corresponding average action potential waveforms. **c**,**f**, Input-output curves showing average number of action potentials elicited by increasing current injections for pyramidal neurons (WT $n = 28$ cells, KO $n = 21$ cells; $P = 0.7057$, 2way ANOVA) and PV+ inhibitory neurons (WT $n = 27$ cells, KO $n = 42$ cells; $P = 0.2993$). Data obtained from current-clamp recordings of neuronal spikes elicited by stimulating with 50 pA step increments, cells clamped at -70mV.

Supplementary Table 1

Passive Membrane Properties

	Pyramidal Neurons		PV Inhibitory Neurons	
Parameters	WT	KO	WT	KO
RMP (mV)	-73.2 ± 2.0	-68.7 ± 2.3	-80.6 ± 1.2	-78.0 ± 0.8
Rin (mOhms)	174.1 ± 18.7	173.5 ± 21.7	93.2 ± 6.3	85.1 ± 4.2
Cm (pF)	96.1 ± 8.1	106.8 ± 12.3	69.8 ± 4.2	80.5 ± 4.5
Tau (ms)	14.7 ± 1.0	16.6 ± 0.9	6.2 ± 0.2	6.4 ± 0.2

Action Potential Features

	Pyramidal Neurons		PV Inhibitory Neurons	
Parameters	WT	KO	WT	KO
Amplitude (mV)	84.9 ± 1.7	82.1 ± 1.9	62.0 ± 2.3	64.5 ± 1.7
Half-width (ms)	1.0 ± 0.1	1.1 ± 0.1	0.3 ± 0.0	0.3 ± 0.0
AHP Amplitude (mV)	-4.5 ± 1.2	-4.0 ± 1.7	-24.0 ± 0.7	-22.1 ± 0.6
Peak to AHP (ms)	3.8 ± 0.5	3.1 ± 0.5	0.8 ± 0.1	0.8 ± 0.0
Threshold (mV)	-39.3 ± 1.0	-37.0 ± 0.9	-39.7 ± 1.0	-41.0 ± 0.9

Table S1: Passive membrane properties and action potential features of WT and KO pyramidal and PV inhibitory neurons. Related to Figure 1.

Supplementary Fig. 3

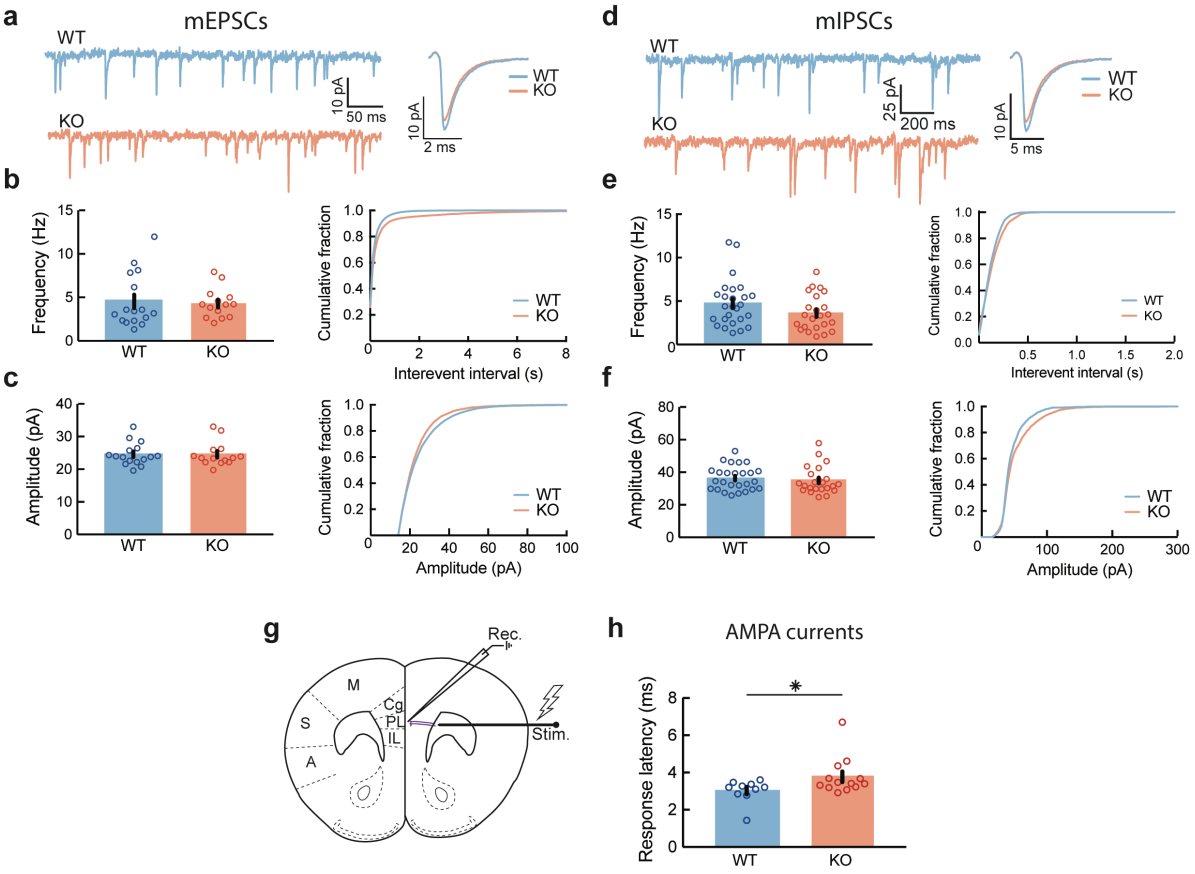

Supplementary Fig. 3 | In Cntnap2 KO mice, no significant alterations in PV+ inhibitory neuron mPSCs but increased stimulus response latency in L2/3 pyramidal neurons. Related to Figure 2. **a-c**, Frequency (WT 4.5 ± 0.8 Hz, KO 4.3 ± 0.5 Hz; $P = 0.9901$, Unpaired t test) and amplitude (WT, 24.5 ± 0.9 pA, KO 24.6 pA ± 1.0; $P = 0.5970$, Wilcoxon test) of mEPSCs (WT $n = 17$, KO $n = 15$) and **d-f**, frequency (WT 4.7 ± 0.5 Hz, KO 3.6 ± 0.4 Hz; $P = 0.4074$, Wilcoxon test) and amplitude (WT 36.0 ± 1.9 pA, KO 37.6 ± 2.5 pA; $P = 0.8238$, Wilcoxon test) of mIPSCs (WT $n = 28$, KO $n = 25$) recorded from parvalbumin-positive (PV) inhibitory neurons are not statistically different between Cntnap2 KO and WT mice. Distribution of data is represented as box and whiskers plots with mean ± SEM. **g**, Monopolar tungsten electrode was used to stimulate long-range axons (purple), which extend from the anterior forceps of the corpus callosum and project onto a patched excitatory neuron in L2/3 mPFC. **h,** Stimulus response onset for L2/3 pyramidal neurons in WT (3.03 ± 0.19 ms; $n = 10$ cells) and KO (3.77 ± 0.28 ms; $n = 13$ cells) mice shows an increase in evoked AMPA current response latency from time stimulus onset (*$P = 0.0438$, Wilcoxon test).

Supplementary Fig. 4

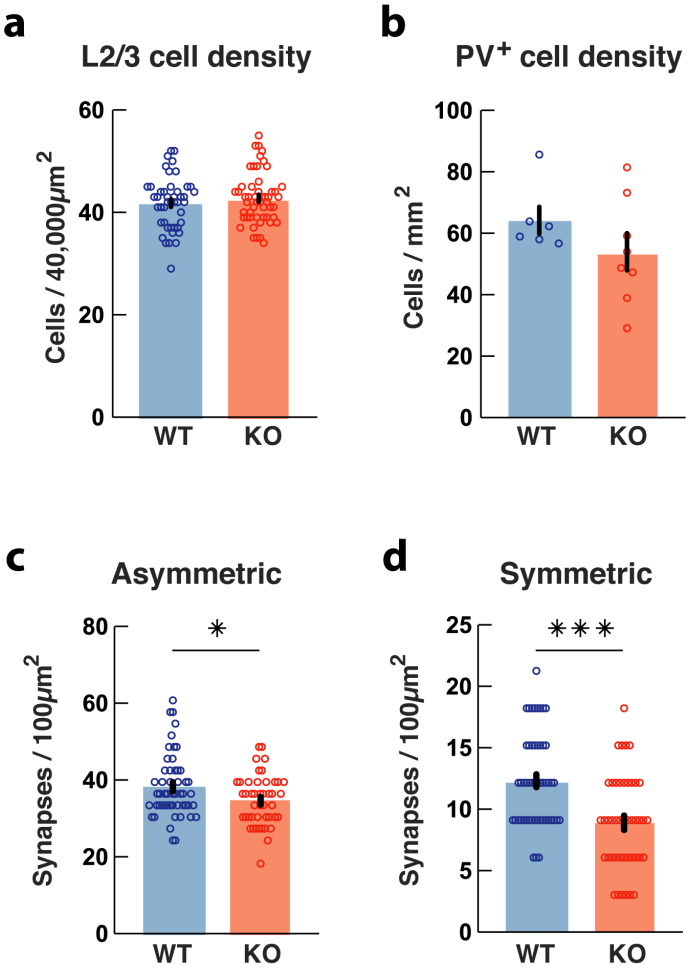

Supplementary Fig. 4. | Cntnap2 KO mice exhibit unaltered L2/3 neuronal cell density and PV+ neuron density but reduced asymmetric (excitatory) and symmetric (inhibitory) synapse density in L1 of prelimbic mPFC. Related to Figure 3. **a.** Prelimbic mPFC L2/3 neuronal density as measured by counting nuclei in n=52 (WT) and n=45 (KO) toluidine blue stained thin sections from n=3 (WT) and n=3 (KO) mice (p=0.36). **b,** Prelimbic PV^+ neuron density as measured by counting immuno-labeled PV^+ neurons in n=6 (WT) and n=8 (KO) sections from n=4 (WT) and n=4 (KO) mice (p=0.23). **c-d,** Graphs showing quantification of asymmetric (putative excitatory: WT 38.26 $\pm$ 1.14 synapses/100 µm^2, *n* = 52 fields; KO 34.63 $\pm$ 0.98 synapses/100 µm^2, *n* = 45 fields; 3 mice per genotype; *P= 0.019, unpaired t-test) and symmetric synapses (putative inhibitory: WT 12.33 $\pm$ 0.52 synapses/100 µm^2, *n* = 52 fields; KO 8.91 $\pm$ 0.58 synapses/100 µm^2, *n* = 44 fields; ****$P < 0.0001$, unpaired t-test).

Supplementary Fig. 5

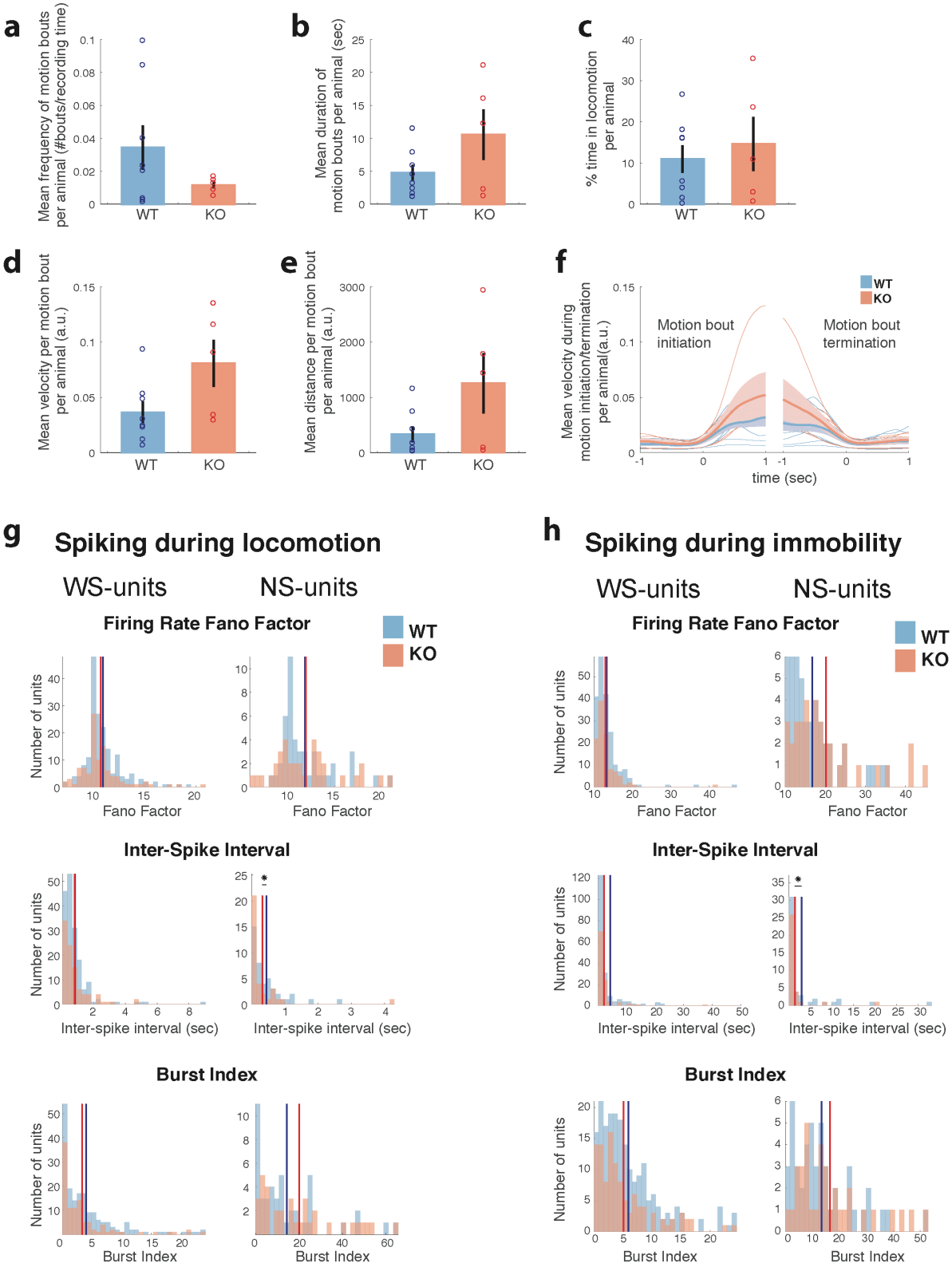

Supplementary Fig. 5 | Comparison of locomotion features and spiking characteristics during both locomotion and immobility between WT and KO single units. Related to Figure 4. **a,** Frequency of motion bouts per animal. **b,** Mean duration per bout. **c,** Percentage time spent in locomotion. **d,** Mean velocity per motion bout. **e,** Mean distance traveled per bout (velocity integral). **f,** Mean velocity per bout during motion initiation and termination. All differences are non-significant ($P > 0.05$; Two-sample t-test, except for panel F, where Wilcoxon test was applied for timesteps where distributions were non-normal by Lilliefors goodness of fit test). **g,** Left column: Wide-spiking units. Right: Narrow-spiking units. Each panel depicts distributions over all WT (blue) and KO (red) unit spiking during locomotion. Lines: Means of corresponding distributions. From top: Firing rate Fano factors (spiking variability), inter-spike intervals and burst indexes. Asterisks: $P < 0.05$, Wilcoxon test, Bonferroni corrected over the two cell types for each measure). Comparing median values yielded similar results (not shown). **h,** Same as **g** for immobility segments.

Supplementary Fig. 6

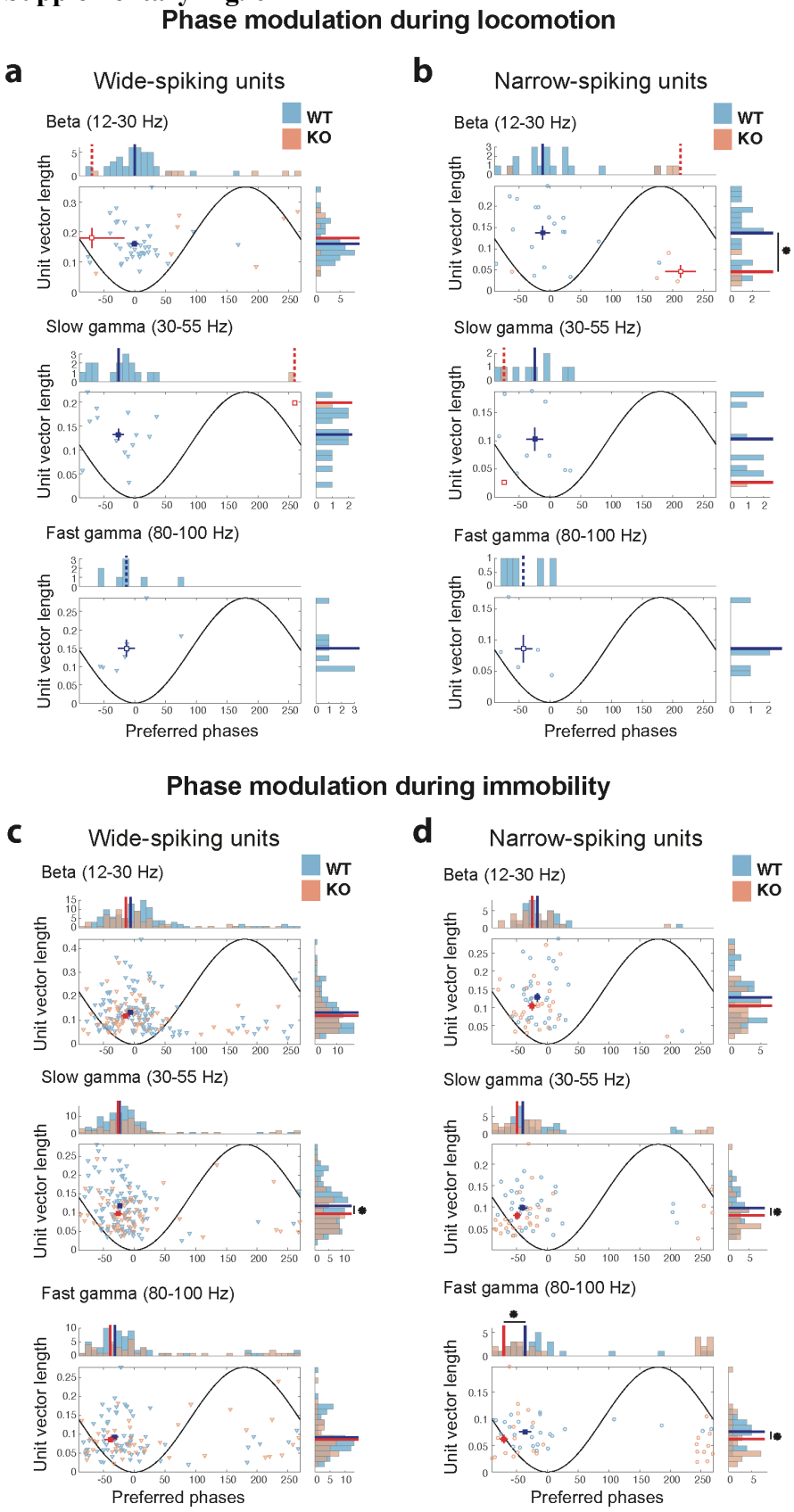

Supplemental Figure 6 | Phase-locking strength and preferred phases of WS and NS units for higher frequency oscillations during locomotion and immobility. Related to Figure 5. **a-b.** Distributions and corresponding histograms of strength of phase-locking (mean vector length) versus preferred phases of pooled WS units (a) and NS units (b) from WT (blue) and KO mice (red). Plotted similarly to Figure 5c. Dashed lines and open rectangles indicate phase means of distributions that are not significantly non-uniform ($P > 0.05$; Rayleigh test for non-uniformity). **c-d.** Same as Figure 5d for all segments of immobility. Both WS and NS units from KO animals exhibit an overall weaker phase locking than those of WT animals (significant mostly in NS units and particularly in higher frequencies).

Supplementary Fig. 7

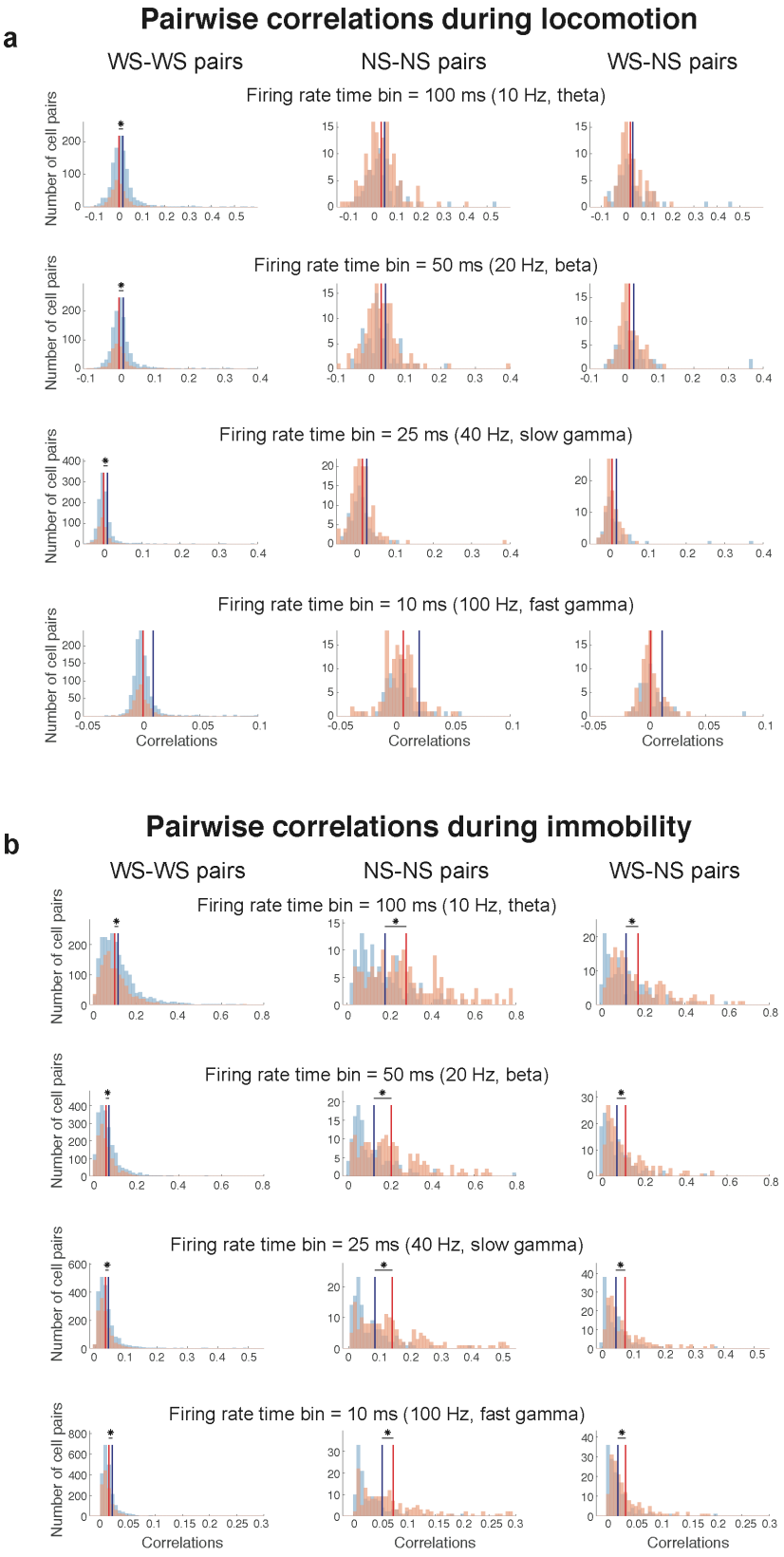

Supplemental Figure 7 | Comparison of firing rate correlations between pairs of WT and KO single units during locomotion and immobility. Related to Figure 5. **a,** Firing rate correlations between pairs of wide-spiking units (left), narrow-spiking units (middle) and wide-narrow spiking unit pairs (right) plotted similarly to Figure 5e. From top: Firing rates per unit pair, computed for locomotion segments over non-overlapping time bins of length: 100ms, 50ms, 25ms, 10ms. Only units with >200 spikes during all motion segments were included. Asterisks: $P < 0.05$, Wilcoxon test, Bonferroni corrected over the 3 unit-type combinations. **b,** Same as **a** for immobility segments.

Supplementary Table 2

Mean number of cells included in phase modulation analysis during locomotion

	Wide-spiking units			Narrow-spiking units		
Frequency	**WT**	**KO**	**P-value**	**WT**	**KO**	**P-value**
1 – 4 Hz (Delta)	10.87 ± 10.19	6 ± 4.95	0.274 (Wilc. test)	3.37 ± 2.82	5.8 ± 4.97	0.292 (t-test)
5 – 11 Hz (Theta)	7.25 ± 7.78	3 ± 2.83	0.192 (Wilc. test)	2.75 ± 2.87	4.2 ± 3.11	0.424 (Wilc. test)
12 – 30 Hz (Beta)	5 ± 8.25	1.4 ± 2.07	0.926 (t-test)	2.25 ± 2.25	0.8 ± 1.30	0.170 (Wilc. test)
30 – 55 Hz (Slow gamma)	2 ± 4.57	0.2 ± 0.45	0.718 (t-test)	1.12 ± 1.55	0.2 ± 0.45	0.391 (t-test)
80 – 100 (Fast gamma)	1 ± 2.45	0 ± 0	0.718 (t-test)	0.62 ± 1.06	0 ± 0	0.391 (t-test)

Mean number of cells included in phase modulation analysis during immobility

	Wide-spiking units			Narrow-spiking units		
Frequency	**WT**	**KO**	**P-value**	**WT**	**KO**	**P-value**
1 – 4 Hz (Delta)	18.62 ± 3.33	18 ± 9.03	0.340 (t-test)	4.75 ± 2.81	6 ± 5.79	0.670 (Wilc. test)
5 – 11 Hz (Theta)	17.12 ± 2.75	16.6 ± 9.127	0.603 (t-test)	4.5 ± 2.51	5.8 ± 5.40	0.635 (Wilc. test)
12 – 30 Hz (Beta)	13.87 ± 7.38	13 ± 6.78	0.832 (Wilc. test)	4.37 ± 2.44	5.6 ± 5.59	0.663 (Wilc. test)
30 – 55 Hz (Slow gamma)	12.62 ± 9.04	12.6 ± 6.98	0.996 (Wilc. test)	4.37 ± 2.56	6.2 ± 5.49	0.516 (Wilc. test)
80 – 100 (Fast gamma)	8.37 ± 7.03	8.8 ± 3.70	0.381 (t-test)	3.12 ± 1.96	5.2 ± 5.26	0.439 (Wilc. test)

Mean number of cells included in correlation analysis

	Wide-spiking units			Narrow-spiking units		
	WT	**KO**	**P-value**	**WT**	**KO**	**P-value**
Locomotion	10.75 ± 11.44	5.8 ± 6.26	0.336 (Wilc. test)	3 ± 2.83	4.4 ± 4.72	0.572 (Wilc. test)
Immobility	20.12 ± 7	19.2 ± 9.88	0.923 (t-test)	4.5 ± 2.45	5.6 ± 5.41	0.686 (Wilc. test)

Table S2: **Mean number of cells included in phase modulation analysis and correlation analysis.** Related to Figure 5.